Supplementary Information (SI) for Journal of Materials Chemistry C.
This journal is © The Royal Society of Chemistry 2025

Supporting Information for

Control of Self-Propagating Reactions and Phases in Ni/Si Reactive Multilayers

Yi-Chen Chen[a], Yuan-Wei Chang[a], Cheng-Chih Hsiang[a], Yi-Pang Chiu[b], Kuan-Wei Su[b], and Yi-Chia Chou[a,*]

[a] Department of Materials Science and Engineering, National Taiwan University, Taipei, 10617, Taiwan

[b] Department of Electrophysics, National Yang Ming Chiao Tung University, Hsinchu, 30010, Taiwan

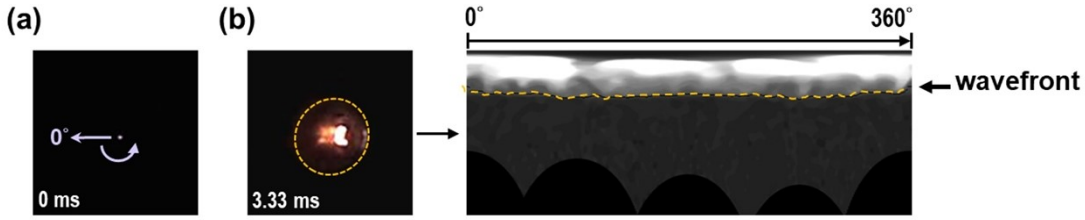

Fig. S1 Calculation of self-propagation velocities. (a) Coordinate transformation; (b) illustration of polar coordinate transformation.

This study used LabVIEW to analyze image sequences from high-speed camera and calculate the self-propagation velocity. To determine the self-propagation velocities, a coordinate transformation was employed. The laser spot of initiation was set as the origin, and the *9 o'clock* position was assigned as *0 degree*, as shown in *Fig. S1 (a)*. Subsequently, the self-propagation wavefront (yellow dashed line) was converted to polar coordinates, with the angle increasing in a counterclockwise direction, as shown in *Fig. S1 (b)*. With increasing time, the first and second wavefronts after the polar-transformation exhibited downward propagation. The self-propagation velocities were determined by linearly fitting the displacement along the propagation time.

Table S1. Self-propagation velocities of RMLs with the bilayer thickness of *50 nm* and *65 nm*. (x: fabrication of samples was not successful)

Bilayer thickness (nm)	Number of bilayers	Total thickness (μm)	Self-propagation velocity (m/s)				
			Flat sample		Rough sample		FR4-based Sample
			1st wavefront	2nd wavefront	1st wavefront	2nd wavefront	2nd wavefront
50	37	1.94	0.55	13.4	x	x	Unable to stimulate
	76	3.34	0.74	14.4	x	x	4.87
	94	5.06	0.95	14.8	0.70	11.0	7.13
	113	6.55	0.96	16.7	0.77	14.7	8.28
	132	6.81	1.18	18.8	0.82	16.7	11.9
	151	8.01	1.21	20.6	0.86	17.3	13.4
65	76	4.86	0.93	11.3	0.56	9.46	3.38
	94	5.98	0.98	14.2	0.64	13.5	6.54
	132	8.47	1.04	17.7	0.72	15.2	10.2

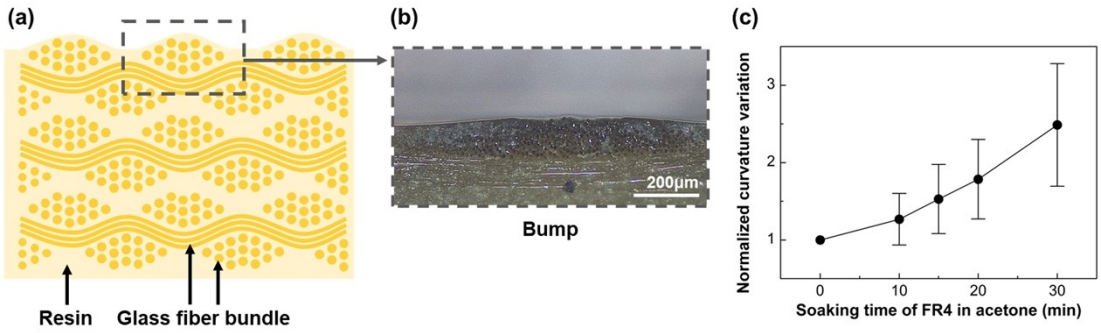

Fig. S2 FR4 structure and acetone-induced morphology changes. (a) Schematic diagram of FR4 composition and structure; (b) optical microscope image of FR4 surface bumps; (c) acetone-induced variations in surface bump curvature.

Figure S1 (a) showed that FR4 was composed of glass fiber bundles and epoxy resin, which had a low thermal conductivity coefficient. The cross-section of FR4 revealed small bumps composed of glass fiber bundles on the surface, as shown in *Figure S1 (b)*. Changes in the surface morphology of FR4 were assessed by measuring the curvature

of the bumps. *Figure S1 (c)* showed that the curvature of bumps increased with soaking time, and the curvature change reached *2.49 times* after soaking for *30 minutes*, confirming that the surface undulation of FR4 increased after soaking in acetone. FR4, being a thermosetting polymer, had a crosslinked network structure formed by its epoxy chains, which resisted solvent erosion. Therefore, after soaking in acetone, FR4 expanded slightly but did not react, resulting in increased surface undulations [1].

References

[1] J. R. Fried, *Polymer science and technology*. Prentice Hall PTR, Englewood Cliffs, N.J, 1995.